

Dynamic Stability of Artificially Sensitive Clay Slopes By Centrifuge Modeling



D.S. Park

K-water Research Institute, Korea Water Resources Corporation, Republic of Korea

B.L. Kutter

University of California, Davis, USA

SUMMARY:

For the very soft sensitive clay deposit, earthquakes can be a major triggering source to cyclic softening and significant deformation. In this study, 8 centrifuge test results for the cement-treated and untreated clay slopes were analyzed to evaluate the effect of sensitivity (S_t) and PGA (peak ground acceleration) on the clay slope failure. Analytic approach using instability factor (N_I) was taken. From analyses, there is a correlation that N_I (the instability factor to cause a slope failure) tends to decrease as sensitivity increases. It indicates that low sensitivity soil can resist a higher demand (higher N_I). Also, N_I decreases as Arias Intensity increases. It indicates that high sensitivity soil is easier to fail for strong earthquake shaking. Because of varying unit weight and slope height as deformation proceeds, equivalent unit weight (γ_e) is introduced and N_I using γ_e to cause a failure is in reasonable agreement with 5.5 shown in the Taylor's chart.

Keywords: Earthquake, Peak ground acceleration, Sensitive clay, Sensitivity, Centrifuge model, Stability number

1. INTRODUCTION

For offshore environment with very soft sensitive clay deposit, earthquakes can be a major triggering source to submarine slides. For onshore site, deformation can be significantly large for sensitive clay slopes in conjunction with liquefiable sand/silt layer as seen in the Turnagain Heights landslide by Alaska earthquake in 1964 (Seed and Wilson 1966, Updike et al. 1988).

In this paper, we examined the effects of sensitivity (S_t) and peak ground acceleration (PGA) on the instability for sensitive clay slopes using geo-centrifuge modeling. An 1-m radius centrifuge at the Center for Geotechnical Modeling at UC Davis served as an equipment to perform the research (Wilson et al. 2010) (Figure 1.1). The advantage of the small centrifuge is the relative ease of operation, providing the ability to conduct a larger number of experiments.

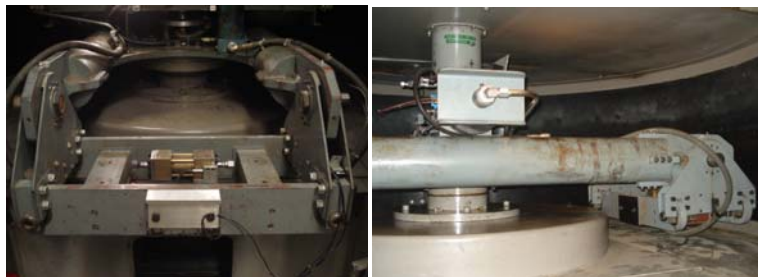


Figure 1.1. UC Davis Schaevitz centrifuge (1m diameter), swing basket and arm assembly

By using cement-treated clay at an appropriate combination of initial water content and cement mixing ratio, we adjusted the target strength level and sensitivity. The experiments were designed to test the following hypotheses:

- $\gamma h/S_u$ to cause instability decreases with S_t increase
- $\gamma h/S_u$ to cause instability decreases with PGA increase

where, γ : unit weight of soil, $\gamma = \gamma_t$ (total unit weight) above the water level, $\gamma = \gamma'$ (buoyant unit weight) below the water table, h : total height of a slope, S_u : undrained strength of soil layer.

The term $\gamma h/S_u$ is the stability factor, which is the inverse form of conventional stability number ($S_u/\gamma h$) used for chart solutions for slope stability (Taylor, 1937). The first hypothesis is come from the common notion that highly sensitive clay is vulnerable to increase of driving force (γh term) or decrease of peak shear strength (S_u). The second hypothesis is led from the idea that higher intensity of earthquake shaking (PGA) can cause deformations even if static loads are small in relation to shear strength.

Table 1.1 summarizes different combinations of total 8 centrifuge tests.

Table 1.1. Centrifuge test program

| ID label | <i>C</i> | <i>W</i> | <i>max</i> <i>G level</i> | γ_t | <i>mild slope</i> <i>angle</i> | <i>steep slope</i> <i>angle</i> |
|-------------------|----------|----------|------------------------------|-------------------|-----------------------------------|------------------------------------|
| | % | % | g | kN/m ³ | deg | deg |
| SFBM C3W135T9 | 3 | 135 | 50 | 13.7 | 8 | 55 |
| SFBM C4W170T7 | 4 | 170 | 50 | 12.9 | 8 | 55 |
| SFBM C4W195T2.4 | 4 | 195 | 50 | 12.6 | 8 | 55 |
| SFBM C4W214C2 | 4 | 214 | 50 | 12.4 | 8 | 55 |
| SFBM C5W220T1 | 5 | 220 | 50 | 12.3 | 8 | 55 |
| Uncemented YL W40 | 0 | 40 | 50 | 17.8 | 8 | 55 |
| YL C2W51T3 | 2 | 51 | 50 | 17.3 | 8 | 55 |
| YL C2W55T3 | 2 | 55 | 50 | 16.3 | 8 | 55 |

Note that SFBM = San Francisco Bay Mud (LL = 88, PI = 50), YL = Yolo Loam (LL = 29, PI = 10), C = cement mixing ratio with respect to the mass of solid of soil, W = initial waters content before cement mixing, γ_t = initial total unit weight

2. MODEL PREPERATION

2.1 Procedure

The raw materials used are a high plasticity clay (Plasticity Index, PI=50), San Francisco Bay Mud (SFBM), and relatively low plasticity (PI=10) silty clay, Yolo Loam (YL). As an additive to make sensitive clay, Type 1 Portland Cement was used. Cement mixing quantities are carefully computed based on measured initial water content and the mass of solid of soil. The required volume of de-ionized water was added and thoroughly mixed to the clay slurry to obtain the desired water content. Then, dry cement was pluviated into the wet clay and mixing was started immediately. For consistency, the soil was mixed for 5 minutes using a stirring tool driven by an electric drill. When mixing was complete, the soft slurry mixed with cement was placed into the transparent-walled rigid centrifuge model container and shaped to the desired slope geometry using spatulas and forms. Sensors were installed at the desired locations as the clay was placed. Figure 2.1 displays a centrifuge model on the arm before and after earthquake events.

General instrumentation layout is composed of multiple accelerometers, pore pressure transducers, and linear potentiometers. Multiple thin, flat sheets of dry pasta were attached on the wall vertically. Based on preliminary practice, this fettuccine pasta proved to be effective to observe the deformed shape after slope failure. After fettuccine noodle attachment, grease was rubbed on the both sides of noodle columns to avoid any penetration of fine clays into the gap between the noodles and the wall. Then, filter paper was folded and placed to fit both the bottom and end walls of the container. Next, a 1 cm layer of dense Nevada sand was pluviated on the bottom uniformly. This bottom sand layer served as a drainage layer. Fettuccine noodles were installed vertically in the soft clay along the centerline of the

container of soil layer after completion of clay placement construction. Noodles were strong enough to penetrate the soft clay.

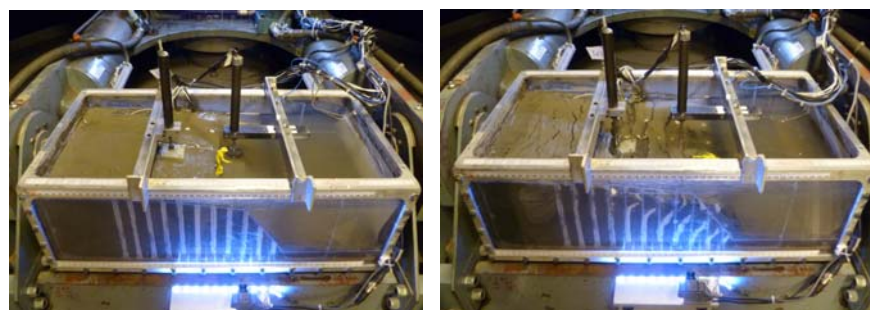


Figure 2.1. Constructed clay slope model before and after dynamic failure (SFBM C4W195T3)

Depending on the spinning schedule and the desired target strength, one to seven days of curing were allowed. After curing, two top stiffeners and linear potentiometers were mounted. Several deformation markers were installed on the surface of slope. In between this process, de-ionized water was filled up to the desired water level in front of the slope. After putting the model on the arm, every sensor cable was connected to right channels according to the instrumentation configuration. The counter-balancing work and checking of sensor signals were performed just before spin-up.

For dynamic tests, the following procedures were taken.

- Start spinning, save static data acquisition, start DVD recording and stopwatch
- Spin up to the target G-level, 50 G, gradually
- Stay for a while at the target G-level watching pore pressure dissipation
- Apply dynamic shaking events
- After final event, coast to stop
- Vane shear tests both for model slopes and vane testing samples
- Dissection in parallel with measurement and taking photos

2.2 Input Motions

Five different earthquake motions were chosen (Table 2.1). After acquiring original acceleration time histories, 4th order band-pass filter were applied to avoid any harmful resonance of centrifuge machine itself. The corner frequencies were 0.8 Hz and 100 Hz. From the commissioning test the natural frequency of Schaevitz machine was estimated to be about 20 Hz at 50 G, which is 0.4 Hz at 1 G condition.

Actual shaking in an in-flight condition started with a small step wave to check shaker's performance. Next, earthquake motions were applied starting from small earthquake motions to the biggest one, the CCSP (Chile) motion. The Loma Prieta, Northridge, and San Fernando motions have durations of 3 to 30 s and similar dominant frequencies. Those three, however, have different levels of peak accelerations. The ChiChi motion was a relatively large earthquake to cause a main failure of slopes. The last and the biggest one, the Chile motion was used to induce a devastating failure, which has a long shaking duration and higher amplitude. Acceleration response spectra of each motion is shown in Figure 2.2.

Table 2.1. Typical input motions applied

| Earthquake | Year | M | Station | Symbol | a_{peak} (g) | duration (s) |
|--------------|------|-----|-------------------------|-----------|----------------|--------------|
| Loma Prieta | 1989 | 6.9 | Monterey City Hall 090 | LP-MCH | 0.063 | 3 |
| Northridge | 1994 | 6.7 | El Monte, LA | NOR-EM | 0.158 | 11 |
| San Fernando | 1971 | 6.6 | Castaic Old Ridge Route | SanF-CORR | 0.324 | 15 |
| ChiChi | 1999 | 7.6 | TCU-W | TCU | 0.444 | 30 |
| Chile | 2010 | 8.8 | Concepcion San Pedro | CCSP | 0.605 | 152 |

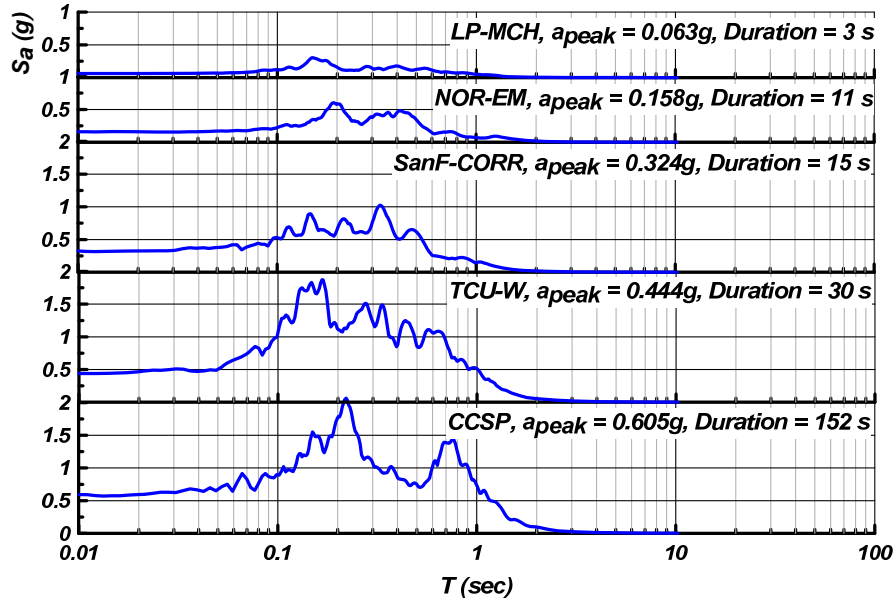


Figure 2.2. Target Acceleration Response Spectra (ARS) of input motions for centrifuge earthquake simulation

3. RESULTS AND ANALYSES

3.1 Basic Observations

A total of 8 dynamic centrifuge tests were performed on artificially cemented sensitive clay slopes and lightly overconsolidated clay. Five tests were composed of high plasticity clay (San Francisco Bay Mud with cement mix ratio of 3 to 5%). The others were composed of low plasticity silty clay (Yolo Loam with cement ratio of 2 to 3%). Two important variables in the experimental study are sensitivity (S_t) and peak ground acceleration (PGA).

Moderate consolidation settlement (about 2 to 4% of slope height on the upslope area for SFBM C5W220, YL C2W51 and YL C2W55) was observed during static centrifuge acceleration. Moderate settlement occurred due to the induced stress gradient and associated consolidation and strength gain with model depth. Linear increase in strength with depth was evident in post-shaking vane shear strength measurements.

Based on data acquisition results, the measured pore pressure ratios (r_u as the ratio of excess pore pressure increase to the vertical effective stress) within clay did not reach values in the range of 70 to 90% which might be expected for NC (normally consolidated) or nearly NC clays subjected to strong shaking due to the effects of high static shear stress and plasticity, and possibly due to time lag associated with measurement of pore pressures in clay and possibly that the sensors were not located in the regions of maximum pore pressure. The max r_u was 33% at 0.59 g of PGA for SFBM C5W220 and 61% at 0.51 g for YL C2W51.

3.2 Shear Strength and Sensitivity

In this study, S_u by vane shear is not constant at all depths as a result of centrifuge spinning. S_u in the model container box was typically taken either at upper part of crest area (~ 25 mm from the surface) or at lower part of crest area (~ 25 mm from the base of clay layer) after stopping centrifuge (Figure 3.1). For the computation of instability factor at failure, representative vane shear strength was taken as the mean value of the two. Because of the curved water table in the centrifuge model, unit weight

should be different above and below the water table. The equivalent unit weight (γ_e) used to compute instability factor was obtained by calculating weighted average value of total and buoyant unit weights considering each volume relative to the impounded water table (Figure 3.2).

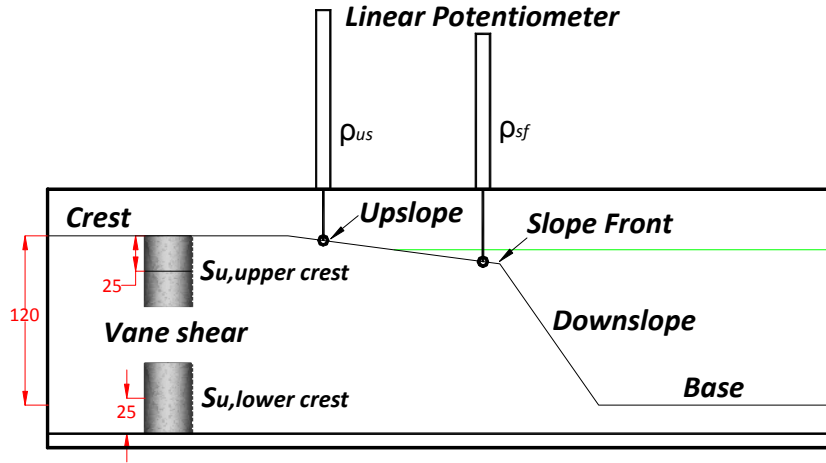


Figure 3.1. Reference locations of measured settlement and shear strength to be used in the analysis

All models indicated the dependence of shear strength on the depth of clay mass. At greater depth, shear strength was always higher than that of the upper layer. In this paper, the shear strength profile was regarded to be linearly proportional to depth. Because of the relatively lower remolded vane shear strength, the sensitivity in the upper area was usually a little higher than the lower layer. For 3 to 5% cement treated SFBM, the distribution of shear strengths applied to this study were about 4 to 21 kPa at lower crest area and S_t varied between about 3 to 12. For 2 to 3% cement treated Yolo Loam, S_t is 8 to 20 and peak strengths were 17 to 120 kPa, depending on cement mixing ratio and initial water content. Untreated Yolo Loam and 3% cement treated SFBM showed low sensitivity (about 2 to 3).

3.3 Analytic Approach

3.3.1 Instability factor

The concept of stability number, N is originated from Taylor's stability chart (1937). Although many updated versions of stability charts have been developed (Baker et al., 2006; Duncan and Wright, 2005), the traditional stability number concept is still in widespread use. Taylor defined the stability number, N for $\phi = 0$ soil, total stress analysis as,

$$N = \frac{c_u}{FS \cdot \gamma \cdot h} = \frac{c_m}{\gamma \cdot h} \quad (3.1)$$

where, c_u : undrained strength of soil, FS: factor of safety, γ : unit weight of soil, h : height of slope, c_m : mobilized shear strength ($c_m = c_u / FS$; factor of safety is regarded as the ratio of shear strength of soil divided by strength being mobilized).

According to Taylor's stability chart, if there is no restriction of base depth, the lower bound of stability number to maintain minimum stability is 0.18 for the slope angle less than 54° . If the slope angle is greater than 53° , Taylor stated that the critical failure surface is always toe circle failure.

Because the instability of clay slope generally increases with the weight of soil mass as a driving force, the inverse form of stability number can be conceptually convenient to understand how unstable the slope is. The "Instability Factor (N_I)" is defined as,

$$N_I = \gamma_e H / S_u \quad (3.2)$$

where, γ_e : equivalent unit weight of soil (defined in Figure 3.2)
H: The total height of a slope in prototype from the top to the base
 S_u : Peak shear strength of clay measured by vane shear.

From Taylor’s stability chart for $\phi = 0$ and slope angle equals to 53° , the upper bound to maintain stability of slope is about 5.52. If the instability factor (N_f) reaches 5.52, the slope is totally unstable when there is no restriction of base depth. For the centrifuge model used, the depth factor, D is about 1.2, which corresponds to 5.5 as the instability factor to be unstable.

3.3.2 Application of Instability Factor

It is useful to clearly define the term, ‘slope failure’ in this study. Two settlement transducers were used on the surface of upslope and slope front area. Failure was deemed to occur when the settlement reaches 5% of the total slope height. In some cases an alternative definition when the settlement is 10% of the slope height was used. Table 3.1 exhibits the G-level or PGA to cause a certain amount of slope settlement.

Table 3.1. G-level or PGA to cause settlements of 2%, 5%, and 10% of slope height

| Model | 2% H | 5% H | 10% H |
|---------------|-----------------|---------------|----------------------------------|
| SFBM C3W135T9 | 24 | 32 | 46 |
| SFBM C4W170T7 | 41 | 50 | Sine wave ($\pm 0.49g$, 1.2Hz) |
| SFBM C4W195T2 | 36 | 43 | 50 |
| SFBM C4W214C2 | 30 | 37 | 46 |
| SFBM C5W220T1 | 50 | TCU (0.543g) | N/A |
| YL C0W40 | 21 | 50 | SanF (0.424g) |
| YL C2W51T3 | LP-MCH (0.065g) | CCSP (0.392g) | N/A |
| YL C2W55T3 | 50 | TCU (0.559g) | CCSP (0.556g) |

In this study, N_f has a different value depending on measured shear strength at different depth. Besides, N_f reduces as slope deformation occurs because of change of slope height (H) and equivalent unit weight (γ_e). Therefore, it is necessary to define slope height, equivalent unit weight, and corresponding N_f to cause a certain deformation at least for both initial and final geometry. From the measured total settlement (ρ_f) and the final height (H_f), equivalent unit weight and slope height at 5% and 10% settlement of slope height can be linearly approximated. Figure 3.2 and Eqns. 3.3 to 3.8 show how to calculate equivalent unit weight and Table 3.2 displays the computed result.

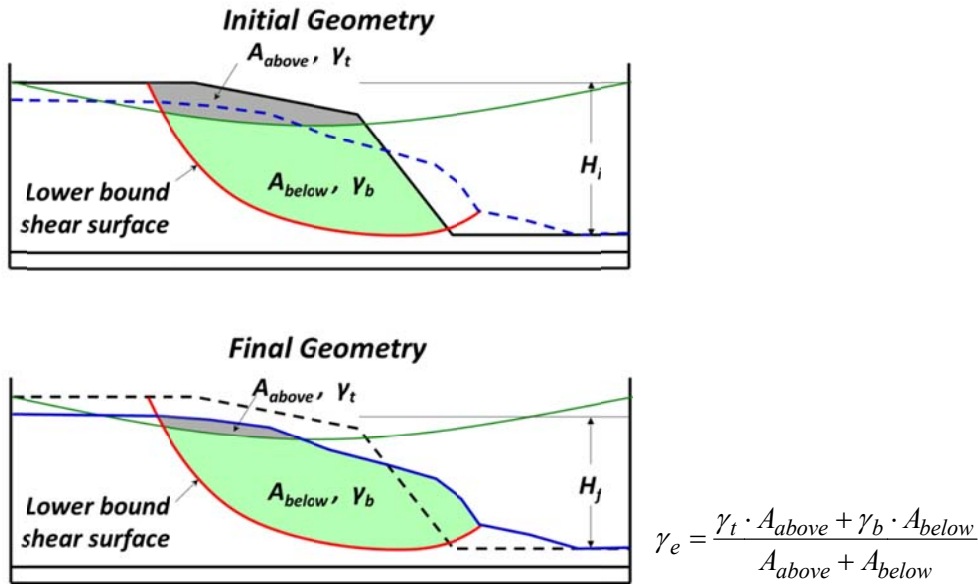


Figure 3.2. Computation of equivalent unit weight for initial and final geometry

$$\gamma_{ei} = \frac{\gamma_t \cdot A_{above} + \gamma_b \cdot A_{below}}{A_{above} + A_{below}} \text{ for initial undeformed geometry} \quad (3.3)$$

$$\gamma_{ef} = \frac{\gamma_t \cdot A_{above} + \gamma_b \cdot A_{below}}{A_{above} + A_{below}} \text{ for final deformed geometry} \quad (3.4)$$

$$\gamma_{e,5\%} = \gamma_{ei} - (\gamma_{ei} - \gamma_{ef}) \cdot \frac{\rho_{5\%}}{\rho_f} \quad (3.5)$$

$$\gamma_{e,10\%} = \gamma_{ei} - (\gamma_{ei} - \gamma_{ef}) \cdot \frac{\rho_{10\%}}{\rho_f} \quad (3.6)$$

$$H_{5\%} = H_i - (H_i - H_f) \cdot \frac{\rho_{5\%}}{\rho_f} \quad (3.7)$$

$$H_{10\%} = H_i - (H_i - H_f) \cdot \frac{\rho_{10\%}}{\rho_f} \quad (3.8)$$

where, γ_{ei} = initial equivalent unit weight for undeformed geometry, γ_{ef} = final equivalent unit weight for deformed geometry, $\gamma_{e,5\%}$ = equivalent unit weight corresponding to the 5% settlement of slope height on the upslope potentiometer, $\gamma_{e,10\%}$ = equivalent unit weight corresponding to the 10% settlement of slope height on the upslope potentiometer, H_i = initial slope height for undeformed geometry, H_f = final slope height for deformed geometry, $H_{5\%}$ = slope height corresponding to the 5% initial slope height, $H_{10\%}$ = slope height corresponding to the 10% initial slope height, ρ_f = final settlement measured on the upslope potentiometer, $\rho_{5\%}$ = 5% upslope settlement with respect to the initial slope height ($\rho_{5\%} = 5\% \cdot H_i$), $\rho_{10\%}$ = 10% upslope settlement with respect to the initial slope height ($\rho_{10\%} = 10\% \cdot H_i$).

Table 3.2. Change of equivalent unit weight and slope height depending on deformation of slope

| Material | γ_{ei} kN/m ³ | γ_{ef} kN/m ³ | H_i mm | H_f mm | $\gamma_{e,5\%}$ kN/m ³ | $\gamma_{e,10\%}$ kN/m ³ | $H_{5\%}$ mm | $H_{10\%}$ mm | $N_{I,5\%}$ | $N_{I,10\%}$ |
|---------------|------------------------------------|------------------------------------|-------------|-------------|---------------------------------------|--|-----------------|------------------|-------------|--------------|
| SFBM C3W135T9 | 9.8 | 7.2 | 120 | 99.4 | 8.8 | 7.9 | 112.4 | 104.9 | 8.0 | 9.6 |
| SFBM C4W170T7 | 3.6 | 5.7 | 120 | 85 | | | | | | |
| SFBM C4W195T2 | 5.9 | 4.3 | 120 | 100.5 | 5.5 | 5.2 | 115.6 | 111.1 | 5.7 | 6.0 |
| SFBM C4W214C2 | 4.6 | 3.1 | 120 | 96.7 | 4.2 | 3.9 | 114.4 | 108.9 | 5.4 | 5.9 |
| SFBM C5W220T1 | 3.9 | 3.1 | 120 | 103.8 | | | | | | |
| YL C0W40 | 9.3 | 8.2 | 120 | 72 | 9.1 | 8.9 | 111.4 | 102.8 | 4.7 | |
| YL C2W51T3 | 9.9 | 8.2 | 120 | 98 | | | | | | |
| YL C2W55T3 | 8.3 | 6.8 | 120 | 98 | | | | | | |

3.3.3 Effects of Instability factor and PGA on Sensitivity

There are two ways for soils to become sensitive in this study. One is from the cement mixing ratio which may represent the degree of cementation. The other is from initial water content. When cement mixing ratio increases, sensitivity increase is mainly governed by increased peak shear strength. But, when the cement mixing ratio is the same, sensitivity is increased by increase of initial water content. When water content increases, the sensitivity increase is mainly governed by reduction of remolded strength.

Figure 3.3 explains the relationship between S_t and $N_{I,5\%,US}$ and $N_{I,10\%,US}$ (instability factor to cause the 5% and 10% settlement of slope height) from the upslope potentiometer (denoted as US). It is observed that $N_{I,5\%,US}$ or $N_{I,10\%,US}$ tends to decrease as sensitivity increases indicating that low

sensitivity soil can resist a higher demand (higher instability factor). More data points would be useful to check if the trend is generally correct since the relationship can be complicated due to the effects of cement mixing ratio, initial water content, and the definition of failure as well as the changing stiffness of soil depending on the sensitivity.

Figure 3.4 presents the relationship of sensitivity and Arias Intensity (I_a) to cause a 5% settlement on the upslope area. Arias intensity (I_a) is applied to quantify the effect of earthquake intensity, duration, and frequency content together (Seed and Wilson, 1967). The calculation is given by,

$$I_a = \frac{\pi}{2g} \int_0^{\infty} (a(t))^2 dt \quad (3.9)$$

where, g : 9.8 m/s², $a(t)$: acceleration time history

Roughly, the Arias Intensity required to cause the 5% settlement decreases as sensitivity increases as expected. More data would be beneficial to convince this pattern in the future.

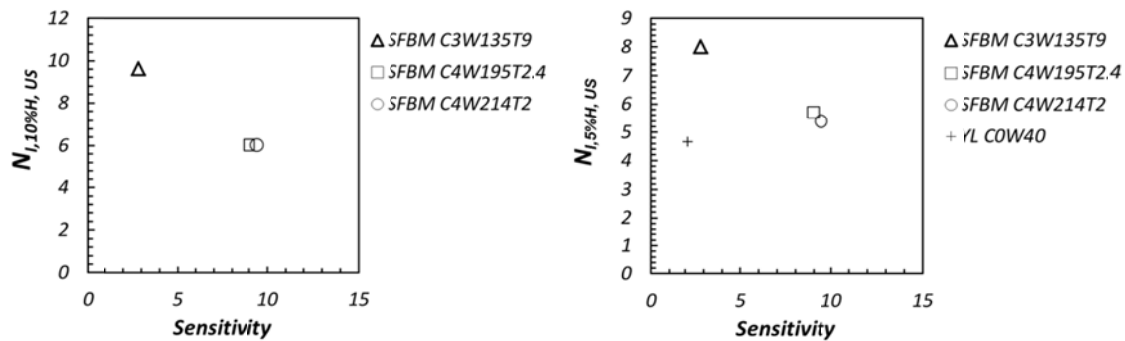


Figure 3.3. A relationship between sensitivity and N_I ($\gamma H / S_u$) to cause a certain deformation.

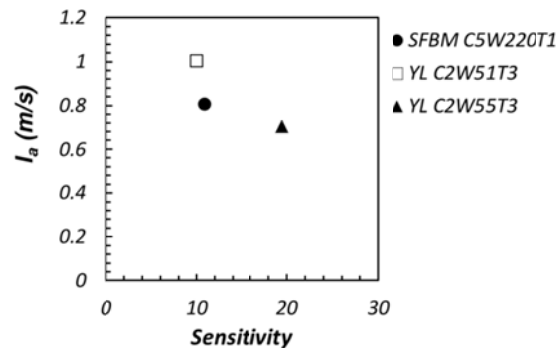


Figure 3.4. A relationship between sensitivity and Arias Intensity (I_a) to cause a 5% settlement on the upslope

4. Conclusions

A total of 8 centrifuge test results for the cement-treated and untreated clay slopes were analyzed to evaluate the effect of sensitivity (S_t) and PGA on the slope failure. Analytic approach using instability factor (N_I ; $\gamma H / S_u$) was taken.

From the test results, there is a weak correlation that $N_{I,5\%,US}$ (the instability factor to cause 5% settlement in the upslope location) and $N_{I,10\%,US}$ tends to decrease as sensitivity increases. It indicates that low sensitivity soil can resist a higher demand (higher instability factor).

Also, $N_{1,5\%,US}$ decreases as Arias Intensity increases as expected. It indicates that high sensitivity soil is easier to fail for strong earthquake shaking.

Because of varying unit weight and slope height as deformation proceeds, it is worthwhile to use equivalent unit weight (γ_e) considering weighted average of γ_t and γ_b with respect to the volume of soil mass above and below the water table. Instability factor using γ_e to cause a failure is in reasonable agreement with 5.5 shown in the Taylor's chart.

ACKNOWLEDGEMENT

The centrifuge testing was performed by the aid of NEES (Network for Earthquake Engineering Simulation) Shared-Use program, NEES@UCD associated with NSF Grant 0530151. Special thanks are extended to professor Jason DeJong and Dr. Dan Wilson for their support at UC Davis.

REFERENCES

- Baker, R., Shukha, R., Operstein, V. and Frydman, S. (2006). Stability charts for pseudo-static slope stability analysis. *Soil Dynamics and Earthquake Engineering* **26:9**, 813-823.
- Duncan, J. M. and Wright, S. G. (2005). Soil strength and slope stability, John Wiley & Sons, Inc.
- Seed, H. B. and Wilson, S. D. (1966). The Turnagain Heights landslide in Anchorage, Alaska. Dept. of Civil Engineering, Institute of Transportation and Traffic Engineering, University of California, Berkeley.
- Taylor, D.W. (1937). Stability of earth slopes. *Journal of Boston Society of Civil Engineers* 24.
- Updike, R. G., Olsen, H. W., Schmoll, H. R., Kharaka, Y. K. and Stokoe, K. H. (1988). Geologic and geotechnical conditions adjacent to the Turnagain Heights landslide, Anchorage, U.S. Geological Survey Bulletin 1817.
- Wilson, D. W., Kutter, B. L. and Boulanger, R. W. (2010). NEES @ UC Davis. *7th International Conference on Physical Modelling in Geotechnics*. Zurich, Switzerland: TC 2, International Society for Soil Mechanics and Geotechnical Engineering.